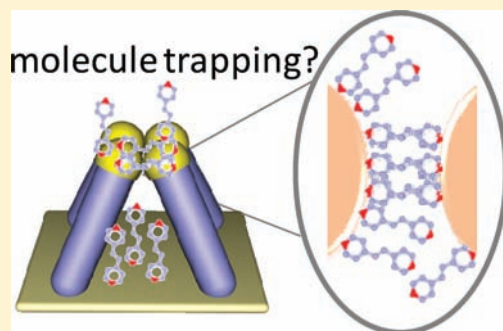


# Study of Molecular Trapping Inside Gold Nanofinger Arrays on Surface-Enhanced Raman Substrates

Ansoon Kim,<sup>†</sup> Fung Suong Ou,<sup>†</sup> Douglas A. A. Ohlberg,<sup>‡</sup> Min Hu,<sup>†</sup> R. Stanley Williams,<sup>‡</sup> and Zhiyong Li<sup>\*,†</sup>

<sup>†</sup>Intelligent Infrastructure Lab, and <sup>‡</sup>nanoElectronics Research Group, Hewlett-Packard Laboratories, 1501 Page Mill Road, Palo Alto, California 94304, United States

**ABSTRACT:** The binding of *trans*-1,2-bis(4-pyridyl)-ethylene (BPE) molecules on substrates arrayed with flexible gold nanofingers has been studied by surface-enhanced Raman spectroscopy (SERS) and angle-resolved X-ray photoelectron spectroscopy (AR-XPS). On the basis of the SERS and XPS results, BPE molecules are found to interact with the gold nanofingers through the lone pair electrons of pyridyl nitrogens, not through delocalized  $\pi$  electrons. Furthermore, after comparing the AR-XPS spectra of finger arrays preclosed before exposure to BPE with the spectra of arrays that closed after exposure to BPE, we observed in the latter case, at grazing takeoff angles, an increase in the component of the nitrogen photoelectron peak associated with pyridyl nitrogen atoms residing on bridging sites. These results demonstrate that a small percentage of BPE molecules was trapped between the neighboring gold finger tips during the finger closing process. However, because these trapped BPE molecules coincidentally resided in the hot spots formed among the touching finger tips, the substantial increase in the observed SERS signal was dominated by the contribution from this small minority of BPE molecules.



## 1. INTRODUCTION

Previously, we reported a simple, yet easily scalable method to make flexible gold nanofinger arrays for SERS applications.<sup>1</sup> The high-density arrays of gold nanofingers were fabricated over a large surface area using nanoimprint lithography (NIL). The flexibility and high aspect ratio of the nanofingers enables the arrays to undergo a self-closing process driven by microcapillary forces during evaporation of the solvent, similar to processes that have been observed in analogous microscale structures.<sup>2–4</sup> These nanofinger structures were applied to SERS, and the estimated enhancement factor (EF) for *trans*-1,2-bis(4-pyridyl)ethylene (BPE) molecules located in the Raman hot spots was  $\sim 2 \times 10^{10}$ .<sup>1</sup> We speculated that the improved EF arose from the incidental creation of self-limiting, sub-nanometer gaps that occurred when molecules were trapped or wedged between the finger tips during the closure process. Subnm gaps are thought to be the source of Raman hot spots with greatly amplified electromagnetic fields under incident laser illumination, and because their contribution to SERS enhancement has been previously studied, both theoretically and experimentally by many groups,<sup>1,5–8</sup> they will not be discussed any further in this Article. Rather, we will focus on the chemical analysis of molecules on the nanofinger surfaces that provides direct physical evidence verifying the active trapping of molecules between finger tips.

Although previous groups have invoked a mechanism involving the trapping of analyte molecules at nanowire junctions (Raman hot spots) to explain the increase of Raman signals observed on touching metal nanowires,<sup>1,9–13</sup> no direct chemical evidence was ever provided to support such a trapping mechanism.

Furthermore, little effort has been devoted to the characterization of the bonding configurations of molecules in the Raman hot spots, which is crucial for a fundamental understanding of both the SERS enhancement mechanism as well as the molecular orientation, in particular, for biological applications.

In this Article, we examined nanofinger substrate surfaces exposed to BPE solutions with SERS and angle-resolved X-ray photoelectron spectroscopy (AR-XPS). Because BPE includes a highly delocalized  $\pi$ -electron system with chemically active pyridyl nitrogen atoms for binding to metal surfaces, it is widely employed as a stable probing molecule to evaluate SERS substrates.<sup>1,14–16</sup> However, little has been reported regarding the bonding configuration of BPE on substrate surfaces. We present here not only the characterization of BPE bonding on our gold finger substrates, but also the verification of BPE trapping between the finger tips by using SERS and AR-XPS measurements.

## 2. EXPERIMENTAL SECTION

**Preparation of Gold Fingers.** As described in our previous report,<sup>1</sup> the finger structures were fabricated using a combination of electron-beam lithography (EBL), reactive ion etching (RIE), and nanoimprint lithography (NIL). A gold film with a nominal thickness of 80 nm was deposited over the polymer fingers by e-beam evaporation. The typical diameter of each finger was 100 nm, and the height was 750 nm.

**SERS Measurements.** *trans*-1,2-Bis(4-pyridyl)-ethylene (BPE, Sigma-Aldrich, 97%) was diluted in ethanol at a concentration of

**Received:** January 25, 2011

**Published:** April 26, 2011

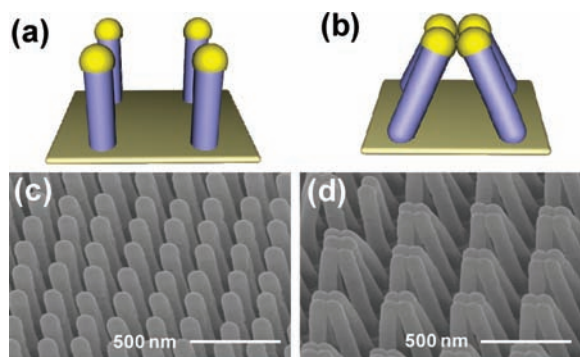


**Figure 1.** Self-closing of gold fingers. Schematic illustrations of (a) as-fabricated and (b) closed fingers; SEM images of (c) as-fabricated and (d) closed fingers.

1 mM as a SERS analyte. To verify the trapping of molecules between closed finger tips, we compared two samples that can be described as (1) BPE-trapped and (2) preclosed fingers. To prepare the BPE-trapped substrate, as-fabricated free-standing fingers were immersed in 1 mM BPE ethanolic solution for 10 min and then air-dried. For the preclosed fingers, the free-standing finger substrate was immersed in pure ethanol solvent and air-dried to induce irreversible finger closing, then reimmersed in the 1 mM BPE solution for 10 min before a final air-dry. Both samples were rinsed with pure ethanol before measurements. SERS measurements were performed using an upright confocal Raman microscope (Horiba Jobin Yvon T64000) equipped with a nitrogen-cooled multichannel CCD detector. A 784.6 nm solid-state laser was used as the excitation source with a measured power of 300  $\mu\text{W}$  at sample surfaces. All spectra were collected with the same micro-Raman setup through a 100 $\times$  objective lens and recorded in the range of 800–1700  $\text{cm}^{-1}$  with a 10 s accumulation time.

**XPS Measurements and Analysis.** X-ray photoelectron spectroscopy (XPS) measurements were performed using a monochromatized Al K $\alpha$  source ( $h\nu = 1486.7$  eV, line width = 0.25 eV), a hemispherical electron energy analyzer (Omicron, Sphera), and a multichannel detector under ultrahigh vacuum (UHV) conditions. The analyzer and X-ray source were configured at 90 $^\circ$  relative to each other. The photoelectron takeoff angles were set at 45 $^\circ$ , 30 $^\circ$ , 20 $^\circ$ , and 10 $^\circ$  with reference to the sample surface. To check sample stability, the spectra taken prior to and after a complete scan were compared. The binding energy (BE) for all spectra was calibrated to the Au 4f $_{7/2}$  peak at 84.00 eV.<sup>17–19</sup> For the analysis of the spectra, peak component fitting (CasaXPS software) was performed using a Shirley background subtraction<sup>20</sup> and asymmetric Voigt functions (mixed Gaussian–Lorentzian), which were obtained from a multilayer BPE XPS spectrum. The fitting parameters were set to reduce the residual standard deviation (STD) of the measured and fitted XPS spectra. The multilayer BPE sample was prepared by repeatedly casting 10 M ethanolic BPE solution on a bare Si substrate and drying in air to form a thick BPE film (>1000  $\mu\text{m}$ ). Charging in the multilayer sample was minimized by use of an electron flood gun during the measurement. The full width half-maximum (fwhm) of the free pyridyl nitrogen components was fixed to 1.2 eV, which was the fwhm of the N 1s component obtained from the multilayer BPE sample.

### 3. RESULTS AND DISCUSSION

Highly ordered, free-standing fingers as fabricated by NIL are shown in Figure 1a and in the SEM image of Figure 1c. After the open fingers were exposed to ethanol and blow-dried with N $_2$  gas, self-closing of the fingers in highly ordered tetramer configurations was observed, as shown in the schematic of Figure 1b and in the SEM image of Figure 1d. If the open fingers are

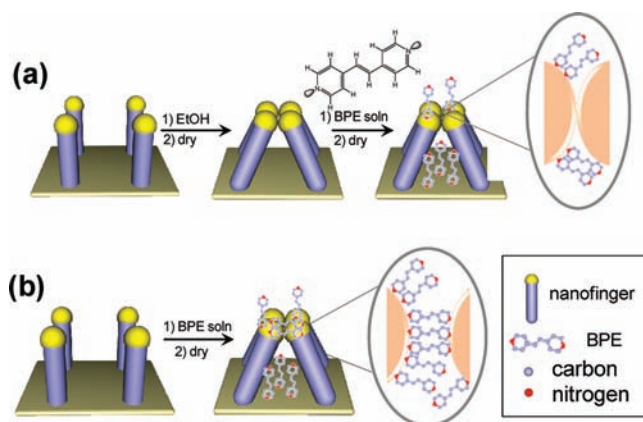


**Figure 2.** Schematic illustrations of the preparation of preclosed and BPE-trapped gold fingers. The inset shows the magnified view of finger tips.

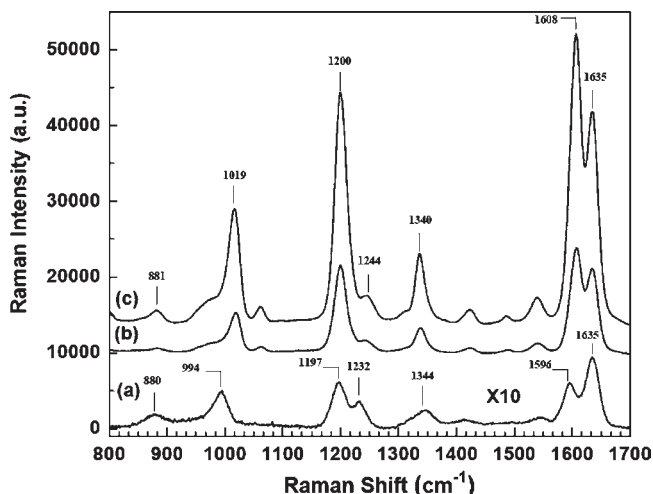


**Figure 3.** Raman spectrum of (a) powder BPE and SERS spectra of (b) preclosed and (c) trapped-BPE fingers. The intensity of the powder spectrum was magnified 10 times.

exposed to a solution containing a target molecule and dried, the flexible fingers can, in theory, close around the molecules and ultimately trap them between closed finger tips. In previous studies<sup>9–11</sup> using touching metal nanowires, it was not clear if the molecules trapped inside the random nanowire bundles were coincident with the hot spots of such bundles. In contrast, the well-defined tetramer aggregates in our nanofinger structures formed predictable hot spots located in the four touching points of the neighboring finger tips.<sup>1</sup> To confirm molecular trapping, we prepared two different samples (preclosed and BPE-trapped fingers), as described in Figure 2. For the preclosed finger substrate (Figure 2a), the free-standing fingers were immersed in pure ethanol, and then blow-dried with N $_2$  gas. After the irreversible formation of the closed fingers, the sample was reimmersed in a 1 mM ethanolic BPE solution for 10 min and air-dried. As shown in Figure 2b, the BPE-trapped fingers were prepared by immersion of the open fingers into the BPE solution before a final air-dry.

We expect that for the BPE-trapped finger substrate, the BPE molecules are trapped between the finger tips, while the

**Table 1. Raman Spectral Peak Assignment of Powder BPE, Preclosed Finger, and BPE-Trapped Finger**

powder	frequency (cm <sup>-1</sup> )		assignments
	preclosed finger	BPE-trapped finger	
880	881	881	$\delta(\text{C}=\text{C})$
994	1016	1019	ring breathing
1197	1200	1200	$\nu(\text{C}-\text{C})_{\text{py}}, \delta(\text{C}-\text{N})_{\text{py}}$
1232	1246	1244	$\delta(\text{C}-\text{H})_{\text{py}}$
1344	1339	1340	$\delta(\text{C}-\text{H}), \delta(\text{C}=\text{C})$
1413	1422	1424	$\delta(\text{C}-\text{H})_{\text{py}}$
1546	1542	1542	$\nu(\text{C}-\text{C})_{\text{py}}, \delta(\text{C}-\text{H})_{\text{py}}, \delta(\text{C}-\text{N})_{\text{py}}$
1596	1607	1608	$\delta(\text{C}-\text{N})_{\text{py}}, \nu(\text{C}-\text{C})_{\text{py}}$
1635	1635	1635	$\nu(\text{C}=\text{C})$

preclosed fingers have no trapped molecules because binding sites between the finger tips are blocked. These differences are illustrated in Figure 2, which schematically depicts a scenario where the amount of BPE molecules in the bridge sites is lower in the preclosed fingers than in the BPE-trapped fingers, while similar amounts of BPE cover the bottom gold surfaces beneath the finger tips of both substrates. Considering the molecular structure of BPE with two pyridine moieties and a vinyl group (Figure 2), we propose that the BPE molecules interact with a gold surface via either the pyridyl nitrogen<sup>15,21,22</sup> or the conjugated  $\pi$  electrons.<sup>22</sup> The two pyridine rings of BPE also allow two possible configurations: either a free-standing orientation involving binding via a single pyridyl nitrogen or a bridging configuration involving binding by both pyridyl nitrogens.

The bonding configurations of BPE on gold have been investigated by comparing the Raman spectrum (Figure 3) of powder BPE with SERS spectra of preclosed and BPE-trapped fingers. The peak assignments are given in Table 1. The observed Raman spectra of the powder and adsorbed BPE are in good agreement with the reported spectra in the literature.<sup>15,23,24</sup> The peak at 994 cm<sup>-1</sup> in the Raman spectrum of the powder BPE (Figure 3a) was assigned to the ring breathing mode of BPE pyridine. This ring breathing mode includes the vibrational movement of the pyridyl nitrogen atoms. It shows a blue-shift by 22 and 25 cm<sup>-1</sup> for the preclosed (Figure 3b) and BPE-trapped (Figure 3c) fingers, respectively. The peak observed at 1596 cm<sup>-1</sup> in the powder spectrum is assigned to the C–N stretching mode of the pyridyl ring, which also includes the movement of the pyridyl nitrogen atoms. This band undergoes a blue-shift of 12 cm<sup>-1</sup> in the SERS spectrum of the BPE-trapped fingers. The blue-shifted peaks in the finger spectra are all associated with the vibrational motions of pyridyl nitrogen, which indicates that the BPE molecules interact with gold via the pyridyl nitrogen atoms. On the other hand, the bands at 880 and 1635 cm<sup>-1</sup> remain unshifted for the powder and finger samples. Both modes involve the vibration of the vinyl group within BPE. If the BPE molecule interacted with gold via  $\pi$  electrons, the conjugation between the aromatic ring and vinyl bond would be disrupted, resulting in a peak shift of the vinyl group. However, the Raman spectra show that this is not the case. Therefore, the BPE molecules must interact with gold via pyridyl nitrogen atoms, not  $\pi$  bonds. In addition, the BPE-trapped fingers exhibit a higher Raman intensity as compared to the preclosed fingers, which is consistent with our

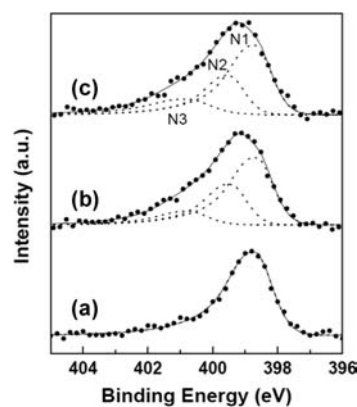


**Figure 4.** N 1s high-resolution XPS spectra of (a) BPE multilayer sample, (b) preclosed fingers, and (c) BPE-trapped fingers. The data were obtained at 45° photoelectron takeoff angle relative to the sample surface. Experimental spectra are shown as dots; solid lines represent best-fit curves; individual fitted components are shown as dashed lines (N1, free nitrogen; N2, weakly adsorbed nitrogen; N3, bridged or strongly adsorbed nitrogen).

previous study.<sup>1</sup> The major difference between the BPE-trapped and the preclosed fingers is most likely the existence of trapped BPE molecules between the finger tips of the former. We therefore speculated that the trapping of BPE molecules between the finger tips is responsible for the higher Raman signal. However, one might equally argue that the preclosure of the fingers in ethanol blocks BPE adsorption sites on the surface of the gold fingers, and hence also results in a lower Raman signal.

To settle this argument, we performed XPS measurements. High-resolution N 1s XPS spectra were obtained at a takeoff angle of 45° relative to the surface for three samples: the BPE multilayer (Figure 4a), the preclosed fingers (Figure 4b), and the BPE-trapped fingers (Figure 4c). All of the N 1s spectra were fitted using the same background and peak shape. To compare the total amounts of adsorbed BPE between the BPE-trapped and preclosed finger substrates, the ratios of the integrated N 1s peak intensity relative to that of Au 4f<sub>7/2</sub> were measured. The N/Au ratio was 0.063 and 0.064 for the BPE-trapped and preclosed finger, respectively, which suggests that roughly the same amount of BPE was adsorbed on both samples. The XPS spectrum of the BPE multilayer shows one peak at 398.7 eV, which is consistent with the reported N 1s XPS results for unmodified pyridine.<sup>21,25,26</sup>

As shown in Figure 4b and c, fitting of the N 1s XPS peaks yields three nitrogen components denoted as N1, N2, and N3. The N1 component in the spectra of the finger samples was observed at a binding energy (BE) of 398.7 eV, which is in perfect agreement with the peak position of the N 1s peak for the multilayer sample. On the basis of the analysis of the BPE multilayer spectrum and previous studies,<sup>21,25,26</sup> we assign the major component (N1) to the nitrogen of unmodified pyridine. In conjunction with our SERS results, the higher binding energy (BE) components, N2 and N3, can be assigned as pyridyl nitrogen atoms of BPE that have interacted with gold. A charge transfer from the lone pair electrons of the pyridyl nitrogen to the gold leads to higher BE of N 1s, which has been observed in previous studies.<sup>21,25,27–29</sup> The N2 component observed at 399.5 eV (0.8 eV higher than the N1 component) is generally assigned to weakly adsorbed pyridyl nitrogen on gold.<sup>25,30–32</sup> The other component N3 was observed at 400.8 eV, which is typical for pyridyl nitrogens adsorbed on gold nanoparticles<sup>25</sup> and



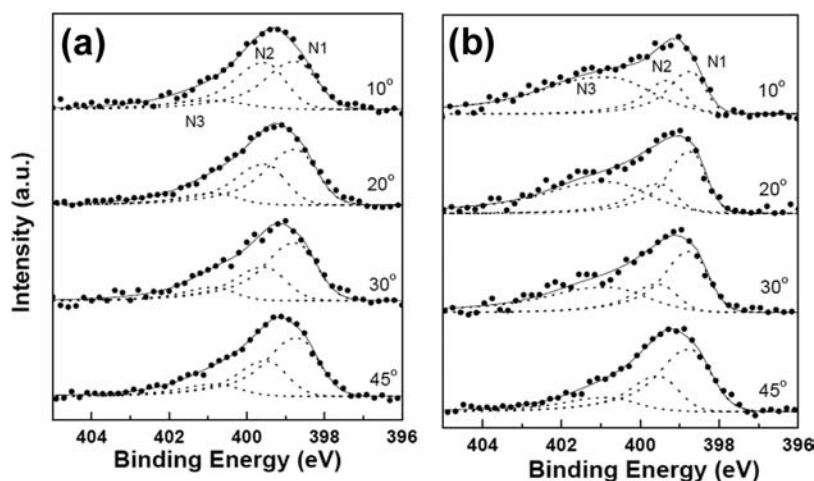


**Figure 5.** Angle-resolved XPS spectra of (a) preclosed and (b) BPE-trapped fingers. The takeoff angles relative to the sample surface are shown in the spectra.

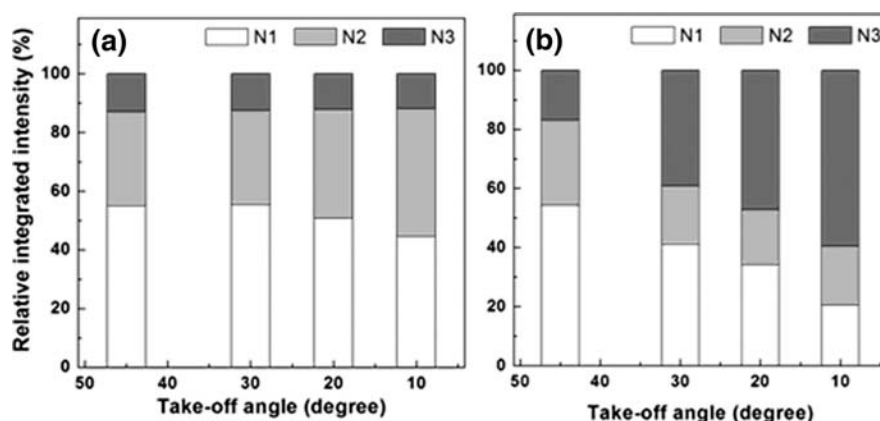


**Figure 6.** Fraction of three N 1s components as a function of takeoff angle for the (a) preclosed and (b) BPE-trapped fingers. The integrated peak intensities of the N1 (white), N2 (light gray), and N3 (dark gray) observed in the AR-XPS spectra (Figure 5) were plotted as a function of takeoff angle.

involved in strong H-bonding.<sup>21</sup> In one instance, a polymer with pyridyl groups coated with gold nanoparticles exhibited the pyridyl nitrogen at a BE of 400.7 eV.<sup>25</sup> Similarly, the strongly H-bonded pyridyl nitrogen has been observed around 400.7 eV.<sup>21</sup> We assign the N3 component to bridged BPE between finger tips or to BPE chemisorbed at one end to gold, which cannot be easily separated by peak-fitting. As compared to BPE, which is weakly adsorbed via one of pyridyl nitrogen atoms, the positively charged nitrogen atoms at both ends of BPE in the bridging configuration are less screened by electron delocalization of highly conjugated  $\pi$  electrons, because the electron delocalization is now split between each pyridyl ring. This should result in a BE of bridged nitrogen that is higher than that of the weakly adsorbed nitrogen. The peak-fitting results indicate that the fraction of the N3 component in the N 1s XPS peak was 13% and 29% for the preclosed and BPE-trapped fingers, respectively. We have to point out here that the ratio of the N3 component to the total N peak area does not necessarily mean that the bridged BPE molecules between the finger tips account for 13% (preclosed fingers) or 29% (trapped fingers) of the total molecules adsorbed on the substrate surfaces, because only a fraction of the N3 component is related to the bridged BPE molecules. Furthermore, two pyridyl nitrogen atoms of each bridged BPE molecule contribute to the N3

peak, whereas only one pyridyl nitrogen contributes to the N1, N2, or N3 component for the free, weakly, and strongly adsorbed BPE molecules, respectively. Finally, it is possible that the sensitivity factor for the photon electrons from the bridged BPE molecules can be much higher than that for the other types of adsorbed BPE molecules. Therefore, the accurate quantification of bridged BPE molecules between the finger tips is still not currently possible. However, the fact that BPE-trapped fingers exhibit a larger amount of N3 qualitatively supports that the molecular trapping is greatly increased if the finger tips undergo closure during exposure to the BPE solution.

To further confirm the BPE trapping in the finger tips, we then performed angle-resolved XPS. Representative N 1s XPS spectra measured at four different takeoff angles of 45°, 30°, 20°, and 10° relative to the surface are shown in Figure 5 for the preclosed and trapped samples. From the AR-XPS spectra, the fraction of the three nitrogen components was plotted for each takeoff angle (Figure 6). For the BPE-trapped fingers, the decrease in the takeoff angle resulted in a more pronounced N3 component. Because measurement at grazing angles provides higher surface sensitivity, the observation of increasing N3 signal with decreasing takeoff angle shows that the bridged or strongly adsorbed BPE molecules are

Table 2. Assignments and Peak-Fitting Results of the N 1s XPS Spectra (Figure 5) Obtained at the Take-off Angle of 10°

suggested assignment	preclosed finger			BPE-trapped finger		
	BE (eV)	relative intensity	fwhm (eV)	BE (eV)	relative intensity	fwhm (eV)
N1 free nitrogen	398.7	45%	1.2	398.7	21%	1.2
N2 weakly adsorbed nitrogen	399.5	43%	1.2	399.3	19%	1.2
N3 bridged or strongly adsorbed nitrogen	400.8	12%	1.8	400.8	60%	2.6

preferably located near the finger tips rather than uniformly distributed all over the finger surfaces. If the N3 component were mainly associated with strongly adsorbed nitrogen via only one of the pyridine rings, one would expect that the N1 component (free pyridyl nitrogen) should increase as the takeoff angle decreases. The reduction of N1 signal with decreasing takeoff angle, as shown in Figure 6, shows that the increase of N3 is associated primarily with bridged BPE molecules. On the other hand, the preclosed fingers exhibit little change in the fraction of the N3 and other nitrogen components at decreasing takeoff angles, which shows that the bonding configurations of BPE molecules on the preclosed fingers are similar everywhere on the substrate. Peak-fitting results of the N 1s XPS spectra measured at a takeoff angle of 10° are shown in Table 2. The N3 width for the preclosed finger (fwhm of 1.8 eV) is narrower than that for the BPE-trapped finger (fwhm of 2.6 eV). We interpret this observation to mean that BPE is only chemisorbed via one nitrogen atom on the preclosed fingers, whereas it is present in both bridged and free-standing configurations for the BPE-trapped substrate. While both species are believed to have roughly the same binding energy, small differences may still exist, and hence generate the broader peak width in the BPE-trapped sample.

Last, on the basis of the XPS data as discussed above, it is clear that a small percentage of the molecules was trapped between the closed finger tips with a bridging configuration in the BPE-trapped sample. Even though the quantification of those trapped molecules was still difficult, the ratio of such trapped molecules to the total BPE molecules adsorbed on the substrate surface can be estimated to be 1:1000 based on the surface area ratio of the touching point over the total tip surface, assuming a monolayer coverage of molecules on the hemispherical metallic tips with a radius of 68 nm. However, the contribution of the trapped BPE molecules to the total SERS signal was significant with almost 3 times more Raman signal as compared to the preclosed sample as shown in Figure 3. Therefore, the trapped molecules showed a further improvement of at least 3 orders of magnitude in the EF as compared to the other molecules on the finger surfaces.

#### 4. CONCLUSIONS

Trapping of *trans*-1,2-bis(4-pyridyl)-ethylene (BPE) on gold finger substrates was investigated by surface-enhanced Raman spectroscopy (SERS) and angle-resolved X-ray photoelectron spectroscopy (AR-XPS). The results indicate that the BPE molecule interacts with the gold through the lone pair electrons of the pyridyl nitrogen, not through delocalized  $\pi$  electrons. The AR-XPS measurements further indicate that the BPE molecules are trapped between the finger tips in a bridging configuration. The results confirm that active and controlled trapping of BPE molecules can be achieved by substrates of flexible gold nano-fingers, and therefore leads to large and reproducible SERS enhancement of the molecules.

#### AUTHOR INFORMATION

##### Corresponding Author

zhiyong.li@hp.com

#### ACKNOWLEDGMENT

We thank Wei Wu and Xuema Li for the assistance with the fabrication process. We also thank John Paul Strachan for the discussion that stimulated this study. This work was partly supported by DARPA.

#### REFERENCES

- (1) Hu, M.; Ou, F. S.; Wu, W.; Naumov, I.; Li, X.; Bratkovsky, A. M.; Williams, R. S.; Li, Z. *J. Am. Chem. Soc.* **2010**, *132*, 12820–12822.
- (2) Chandra, D.; Yang, S. *Langmuir* **2009**, *25*, 10430–10434.
- (3) Kondo, T.; Juodkazis, S.; Misawa, H. *Appl. Phys. A: Mater. Sci. Process.* **2005**, *81*, 1583–1586.
- (4) Goldfarb, D. L.; de Pablo, J. J.; Nealey, P. F.; Simons, J. P.; Moreau, W. M.; Angelopoulos, M. *J. Vac. Sci. Technol., B* **2000**, *18*, 3313–3317.
- (5) Wustholz, K. L.; Henry, A. I.; McMahon, J. M.; Freeman, R. G.; Valley, N.; Piotti, M. E.; Natan, M. J.; Schatz, G. C.; Duynne, R. P. V. *J. Am. Chem. Soc.* **2010**, *132*, 10903–10910.
- (6) Jiang, J.; Bosnick, K.; Maillard, M.; Brus, L. *J. Phys. Chem. B* **2003**, *107*, 9964–9972.
- (7) Lim, D. K.; Jeon, K. S.; Kim, H. M.; Nam, J. M.; Suh, Y. D. *Nat. Mater.* **2010**, *9*, 60–67.
- (8) McMahon, J. M.; Henry, A. I.; Wustholz, K. L.; Natan, M. J.; Freeman, R. G.; Van Duynne, R. P.; Schatz, G. C. *Anal. Bioanal. Chem.* **2009**, *394*, 1819–1825.
- (9) Lee, S. J.; Morrill, A. R.; Moskovits, M. *J. Am. Chem. Soc.* **2006**, *128*, 2200–2201.
- (10) Schierhorn, M.; Lee, S. J.; Boettcher, S. W.; Stucky, G. D.; Moskovits, M. *Adv. Mater.* **2006**, *18*, 2829–2832.
- (11) Sauer, G.; Brehm, G.; Schneider, S.; Graener, H.; Seifert, G.; Nielsch, K.; Choi, J.; Goring, P.; Gosele, U.; Miclea, P. *Appl. Phys. Lett.* **2006**, *88*, 023106.
- (12) Wu, Y.; Livneh, T.; Zhang, Y. X.; Cheng, G.; Wang, J.; Tang, J.; Moskovits, M.; Stucky, G. D. *Nano Lett.* **2004**, *4*, 2337–2342.
- (13) Kang, T.; Yoon, I.; Jeon, K. S.; Choi, W.; Lee, Y.; Seo, K.; Yoo, Y.; Park, Q. H.; Ihee, H.; Suh, Y. D. *J. Phys. Chem. C* **2009**, *113*, 7492–7496.
- (14) Felidj, N.; Aubard, J.; Levi, G.; Krenn, J. R.; Hohenau, A.; Schider, G.; Leitner, A.; Aussenegg, F. R. *Appl. Phys. Lett.* **2003**, *82*, 3095–3097.
- (15) Zhuang, Z.; Cheng, J.; Jia, H.; Zeng, J.; Han, X.; Zhao, B.; Zhang, H.; Zhang, G.; Zhao, W. *Vib. Spectrosc.* **2007**, *43*, 306–312.
- (16) Freeman, R. G.; Grabar, K. C.; Allison, K. J.; Bright, R. M.; Davis, J. A.; Guthrie, A. P.; Hommer, M. B.; Jackson, M. A.; Smith, P. C.; Walter, D. G. *Science* **1995**, *267*, 1629.
- (17) Lindau, I.; Pianetta, P.; Yu, K. Y.; Spicer, W. E. *Phys. Rev. B* **1976**, *13*, 492–495.
- (18) McLean, W.; Colmenares, C. A.; Smith, R. L.; Somorjai, G. A. *J. Phys. Chem.* **1983**, *87*, 788–793.

- (19) Anthony, M. T.; Seah, M. P. *Surf. Interface Anal.* **1984**, *6*, 95–106.
- (20) Shirley, D. A. *Phys. Rev. B* **1972**, *5*, 4709–4714.
- (21) Zubavichus, Y.; Zharnikov, M.; Yang, Y.; Fuchs, O.; Umbach, E.; Heske, C.; Ulman, A.; Grunze, M. *Langmuir* **2004**, *20*, 11022–11029.
- (22) Gandubert, V. J.; Lennox, R. B. *Langmuir* **2005**, *21*, 6532–6539.
- (23) Sun, G.; Grundmeier, G. *Thin Solid Films* **2006**, *515*, 1266–1274.
- (24) Felidj, N.; Truong, S. L.; Aubard, J.; Levi, G.; Krenn, J. R.; Hohenau, A.; Leitner, A.; Aussenegg, F. R. *J. Chem. Phys.* **2004**, *120*, 7141–7146.
- (25) Liu, W.; Yang, X.; Xie, L. *J. Colloid Interface Sci.* **2007**, *313*, 494–502.
- (26) Zhou, X.; Goh, S. H.; Lee, S. Y.; Tan, K. L. *Appl. Surf. Sci.* **1998**, *126*, 141–147.
- (27) Behzadi, B.; Ferri, D.; Baiker, A.; Ernst, K. H. *Appl. Surf. Sci.* **2007**, *253*, 3480–3484.
- (28) Silien, C.; Buck, M.; Goretzki, G.; Lahaye, D.; Champness, N. R.; Weidner, T.; Zharnikov, M. *Langmuir* **2009**, *25*, 959–967.
- (29) Bili, A.; Reimers, J. R.; Hush, N. S. *J. Phys. Chem. B* **2002**, *106*, 6740–6747.
- (30) Wandlowski, T.; Ataka, K.; Mayer, D. *Langmuir* **2002**, *18*, 4331–4341.
- (31) Cai, W. B.; Wan, L. J.; Noda, H.; Hibino, Y.; Ataka, K.; Osawa, M. *Langmuir* **1998**, *14*, 6992–6998.
- (32) Frank, K. H.; Dudde, R.; Koch, E. E. *Chem. Phys. Lett.* **1986**, *132*, 83–87.